

# Multiple passages of light through an absorption inhomogeneity in optical imaging of turbid media

M. Xu, W. Cai, and R. R. Alfano

*Institute for Ultrafast Spectroscopy and Lasers, New York State Center of Advanced Technology for Ultrafast Photonic Materials and Applications, and Department of Physics, The City College and Graduate Center of the City University of New York, New York, New York 10031*

Received March 24, 2004

Multiple passages of light through an absorption inhomogeneity of finite size deep within a turbid medium are analyzed for optical imaging by use of the self-energy diagram. The nonlinear correction becomes more important for an inhomogeneity of a larger size and with greater contrast in absorption with respect to the host background. The nonlinear correction factor agrees well with that from Monte Carlo simulations for cw light. The correction is approximately 50%–75% in the near infrared for an absorption inhomogeneity with the typical optical properties found in tissues and five times the size of the transport mean free path. © 2004 Optical Society of America

OCIS codes: 290.4210, 290.7050, 170.3660.

The main objective of optical imaging of turbid media is to locate and identify the embedded inhomogeneities by essentially inverting the difference in photon transmittance in the time or frequency domains due to the presence of these inhomogeneities.<sup>1–4</sup> The key quantity involved is the Jacobian, which quantifies the influence on the detected signal due to the change of the optical parameters of the medium. The linear perturbation approach is suitable for calculating the Jacobian for only a small and weak absorption inhomogeneity and is not valid when the absorption strength is large.<sup>5</sup> This failure can be attributed to the multiple passages through the abnormal site by the photon. The most important correction is the self-energy correction,<sup>6</sup> which takes into account the repeated visits made by a photon through the site up to an infinite number of times. The presence of other inhomogeneity islands can be ignored because the photon propagator decreases rapidly with the distance between two separate sites.

In this Letter the nonlinear correction for an absorption inhomogeneity of a large strength due to repeated visits by the photon is modeled by a nonlinear correction factor (NCF) to the linear perturbation approach. The NCF as a function of the size and the strength of the inhomogeneity is estimated by use of the self-energy diagram. The NCF is obtained from the cumulant approximation to the radiative transfer and verified by Monte Carlo simulations for cw light. The magnitude of the NCF is 0.5–1 for an absorptive inhomogeneity of up to  $5l_t$  ( $l_t$  is the mean transport free path of light) and of the typical optical properties of human tissues ( $\mu_a l_t / c \sim 0.01$ – $0.05$ , where  $\mu_a$  is the absorption coefficient and  $c$  is the speed of light in the medium).

If we consider an absorption site centered at  $\bar{\mathbf{r}}$  and far away from both the source and the detector, change in detected light  $\Delta I$  at detector  $\mathbf{r}_d$  from a modulated point source at  $\mathbf{r}_s$  including the multiple passages through the site is given by

$$\begin{aligned} \Delta I &= -G(\mathbf{r}_d, \omega | \bar{\mathbf{r}}) V \delta \mu_a(\bar{\mathbf{r}}) \sum_{n=0}^{\infty} [-\bar{N}_{\text{self}}(\omega; R) V \delta \mu_a(\bar{\mathbf{r}})]^n \\ &\quad \times G(\bar{\mathbf{r}}, \omega | \mathbf{r}_s) \\ &= -G(\mathbf{r}_d, \omega | \bar{\mathbf{r}}) \frac{V \delta \mu_a(\bar{\mathbf{r}})}{1 + \bar{N}_{\text{self}}(\omega; R) V \delta \mu_a(\bar{\mathbf{r}})} \\ &\quad \times G(\bar{\mathbf{r}}, \omega | \mathbf{r}_s), \end{aligned} \quad (1)$$

where  $\delta \mu_a$  is the excess absorption of the absorption site of size  $R$  and volume  $V$ ,  $\omega$  is the modulation frequency of light,  $G$  is the propagator of photon migration in the background medium, and

$$\bar{N}_{\text{self}}(\omega; R) = \frac{1}{V^2} \int_V \int_V G(\mathbf{r}_2, \omega | \mathbf{r}_1) d^3 \mathbf{r}_2 d^3 \mathbf{r}_1 \quad (2)$$

is the self-propagator that describes the probability that a photon revisits volume  $V$ . Here  $G(\mathbf{r}_2, \omega | \mathbf{r}_1)$  gives the probability density that a photon leaves the volume at  $\mathbf{r}_1$  and reenters it at  $\mathbf{r}_2$ . The scattering property of the site is the same as that of the background. In Eq. (1)  $G(\mathbf{r}_d, \omega | \bar{\mathbf{r}})$  and  $G(\bar{\mathbf{r}}, \omega | \mathbf{r}_s)$  are well modeled by the center-moved diffusion model as long as separations  $|\mathbf{r}_d - \bar{\mathbf{r}}|$  and  $|\mathbf{r}_s - \bar{\mathbf{r}}|$  are much greater than  $l_t$ .<sup>7</sup> However, the diffusion Green's function cannot be used in Eq. (2) to evaluate  $\bar{N}_{\text{self}}(\omega; R)$  because the diffusion approximation breaks down when  $\mathbf{r}_1$  is in the proximity of  $\mathbf{r}_2$ .

Comparing Eq. (1) with the standard linear perturbation approach, the nonlinear multiple passage effect of an absorption site is represented by a NCF:

$$\text{NCF} = [1 + \bar{N}_{\text{self}}(\omega; R) V \delta \mu_a(\bar{\mathbf{r}})]^{-1}. \quad (3)$$

This factor serves as a universal measure of the nonlinear multiple-passage effect as long as the absorption site is far from both the source and the detector and its size is much smaller than its distance to both the source and the detector. This correction is more significant when the NCF is further away from unity.

Photon propagator  $N(\mathbf{r}_2, t | \mathbf{r}_1, \mathbf{s})$ , the probability that a photon propagates from position  $\mathbf{r}_1$  with propagation direction  $\mathbf{s}$  to position  $\mathbf{r}_2$  in time  $t$ , for any separation between  $\mathbf{r}_1$  and  $\mathbf{r}_2$ , was recently derived<sup>7,8</sup> in the form of a cumulant approximation to the radiative transfer.

In the case of interest in which the absorption site is deep inside the medium, the photon distribution is isotropic. The photon propagator is simplified to  $N_{\text{eff}}(r, t) \equiv N_{\text{eff}}(|\mathbf{r}_2 - \mathbf{r}_1|, t)$ , which is obtained by averaging  $N(\mathbf{r}_2, t | \mathbf{r}_1, \mathbf{s})$  over the propagation direction  $\mathbf{s}$  of light over the  $4\pi$  solid angle. In the frequency domain this effective propagator is approximately given by

$$N_{\text{eff}}(r, \omega) \approx \begin{cases} \frac{1}{4\pi r^2 c} \exp\left(-\frac{1}{3} \kappa^2 l_t r\right) \\ + \frac{\exp(-\kappa l_t)}{4\pi D r \kappa l_t} \sinh(\kappa r), & r < l_t, \\ \frac{\exp(-\kappa r)}{4\pi D r \kappa l_t} \sinh(\kappa l_t), & r \geq l_t \end{cases} \quad (4)$$

where  $D \equiv l_t c/3$  and  $\kappa \equiv [3(\mu_a - i\omega)/l_t c]^{1/2}$ , whose sign is chosen with a nonnegative real part. The two terms in  $N_{\text{eff}}$  when  $r < l_t$  represent ballistic and diffusion contributions, respectively. The ballistic term does not depend on scattering because the photon distribution involved is already isotropic. Only diffusion contributes to  $N_{\text{eff}}$  when  $r > l_t$ . The self-propagator for an absorption sphere deep inside the medium is given by

$$\begin{aligned} \bar{N}_{\text{self}}(\omega; R) &= \frac{1}{V^2} \int_V \int_V N_{\text{eff}}(|\mathbf{r}_2 - \mathbf{r}_1|, \omega) d^3 \mathbf{r}_2 d^3 \mathbf{r}_1 \\ &= \frac{1}{V} \int_0^{2R} N_{\text{eff}}(r, \omega) \gamma_0(r) 4\pi r^2 dr, \end{aligned} \quad (5)$$

where  $\gamma_0(r) = 1 - (3r/4R) + (1/16)(r/R)^3$  is the characteristic function for a uniform sphere.<sup>9</sup> An absorption site of an arbitrary shape can be treated the same way. The exact self-propagator must be computed by a numerical quadrature. A good approximation of  $\bar{N}_{\text{self}}(\omega; R)$  is

$$\bar{N}_{\text{self}}(\omega; R) = \frac{l_t}{Vc} \times \begin{cases} \left( \frac{3}{4} \xi + \xi^3 \right) - \xi^3 \kappa l_t + \mathcal{O}(\kappa^2), & \xi \leq 1/2 \\ \left( \frac{6}{5} \xi^2 + \frac{1}{2} - \frac{3}{16} \xi^{-1} + \frac{3}{320} \xi^{-3} \right) \\ - \xi^3 \kappa l_t + \mathcal{O}(\kappa^2), & \xi > 1/2 \end{cases} \quad (6)$$

by use of relation (4), where  $\xi \equiv R/l_t$  when  $|\kappa|R \ll 1$ . The exact and approximate versions of dimensionless self-propagator  $\bar{N}_{\text{self}} V l_t^{-1} c$  when  $\kappa = 0$  are plotted as solid and dashed curves, respectively, in Fig. 1(a). Dimensionless self-propagator  $\bar{N}_{\text{self}} V l_t^{-1} c$  depends solely on two dimensionless quantities  $\kappa l_t$  of the background and  $R/l_t$  of the absorbing sphere.

It is worthwhile to point out that the self-propagator in time  $\bar{N}_{\text{self}}(t; R)$ , the inverse Fourier transform of

Eq. (5), includes the contribution from the ballistic motion of the photon when the photon passes through the site. This ballistic contribution manifests itself as the linear decay of  $N_{\text{self}}(t; R)V$  in the form of  $\gamma_0(ct)$  near the origin of the time, followed by a transition to diffusion [Fig. 1(b)].

The NCF is obtained by plugging Eq. (5) or (6) into Eq. (3). In particular, we have

$$\text{NCF} \approx \begin{cases} \left[ 1 + \frac{9}{16\pi} q \left( \xi^{-2} + \frac{4}{3} \right) \right]^{-1}, & \xi \leq 1/2 \\ \left[ 1 + \frac{9}{10\pi} q \left( \xi^{-1} + \frac{5}{12} \xi^{-3} \right) \right. \\ \left. - \frac{5}{32} \xi^{-4} + \frac{1}{128} \xi^{-6} \right]^{-1}, & \xi > 1/2 \end{cases} \quad (7)$$

where  $q \equiv V \delta \mu_a(\bar{\mathbf{r}})/l_t^2 c$  is the dimensionless strength of the absorber when  $|\kappa|R \ll 1$ . For an absorber of fixed  $q > 0$ , the effectiveness of absorbing light is diminished (the NCF decreases) when its size is reduced. This can be understood from the fact that the photon spends less time per volume inside the absorber of a smaller dimension because of the ballistic motion of the photon after each scattering event. The photon leaves a small site ( $R < l_t$ ) in an almost straight line. The diffusion behavior for an individual photon is observed only after a large number of scattering and on a scale larger than  $l_t$ .

Figure 2 shows plots of the NCF versus absorber size for typical absorbers of excess absorption  $\delta \mu_a l_t/c$  equal to 0.01 and 0.05. The nonlinear correction factor generally decreases with the size of the absorber whose excess absorption is fixed. With the increase of the background absorption and the modulation frequency, the nonlinear correction becomes less accentuated. The phase delay is larger for higher modulation frequencies and less background absorption.

Monte Carlo simulations<sup>10</sup> are performed for cw light propagating in a uniform nonabsorbing and isotropic scattering slab. The thickness of the slab is  $L = 80l_t$ . A spherical absorber of radius  $R$  is located at the center  $(0, 0, L/2)$  of the slab. The excess absorption of the absorber is  $\delta \mu_a l_t/c = 0.01$ . The absorber has the same scattering property as the background. The details of the Monte Carlo computation were provided in a previous publication.<sup>11</sup> The correlated sampling method

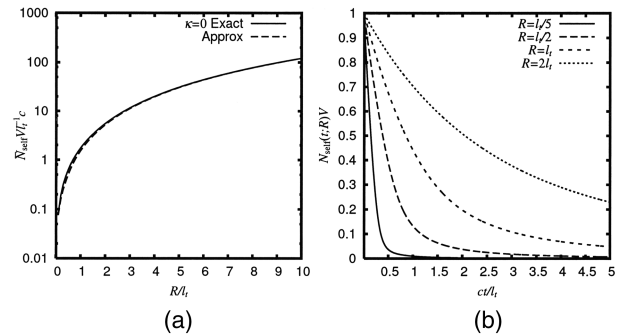


Fig. 1. (a) Self-propagator  $\bar{N}_{\text{self}}(\omega; R) V l_t^{-1} c$  and its approximation form when  $\kappa = 0$ . (b) Self-propagator for spheres of various radii in the time domain inside a nonabsorbing medium.

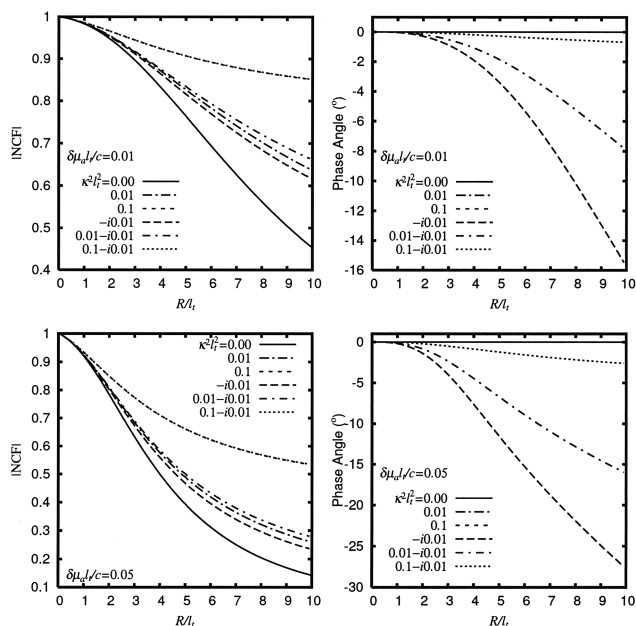


Fig. 2. NCF (magnitude and phase angle) versus the size of absorbers whose excess absorption  $\delta\mu_a l_t/c$  equals 0.01 and 0.05. Note that  $\kappa^2 l_t^2 = 3(\mu_a - i\omega)l_t/c$  for the background medium.

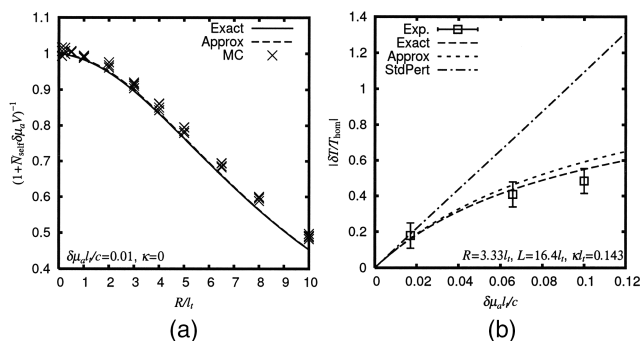


Fig. 3. (a) Theoretical nonlinear correction factors from numerical quadrature (Exact), the approximate form of relation (7) (Approx), and Monte Carlo simulations (MC). Results from four independent Monte Carlo simulations are shown for each radius. The standard linear perturbation approach corresponds to horizontal line NCF = 1 (not shown in the figure). (b) Percentage change of the cw transmittance from the experimental data given in Fig. 9 of Ref. 5 compared with the theoretical predictions made by the standard linear perturbation approach (StdPert) and those including NCF (Exact and Approx).

is used in each simulation to reduce variance.<sup>12</sup> A single simulation is used to compute the change in light transmittance due to the presence of the absorption site and the corresponding NCF. Figure 3(a) shows the NCFs obtained from numerical quadrature, the approximate form of relation (7), and Monte Carlo simulations. The agreement between our theoretical NCF and that from Monte Carlo simulations is excellent. The slight difference between them at large radii is accounted for by the fact that the sphere can no longer

be regarded as small compared with the dimensions of the slab.

Figure 3(b) shows the percentage change of the cw transmittance estimated from the experimental data given in Fig. 9 of Ref. 5. The relevant parameters of the experiment are summarized in the inset. The theoretical predictions from the linear perturbation approach with and without the nonlinear correction are also shown in Fig. 3(b), assuming a collimated point source and a point detector in a confocal setup. Our theoretical prediction with nonlinear correction provides a significant improvement over linear perturbation and agrees much better with the experimental result.

The typical value of the absorption coefficient of human tissues in the near infrared indicates that  $\mu_a l_t/c \sim 0.01-0.05$ .<sup>13,14</sup> This fact should put our results on NCFs in this range (Figs. 2 and 3) into perspective. The nonlinear correction becomes more important for an inhomogeneity of a larger size and with greater contrast in absorption with respect to the background. The value of the NCF decreases from  $\sim 0.75$  to  $\sim 0.5$  for an absorption site of radius  $5l_t$  with excess absorption  $\delta\mu_a l_t/c$  increasing from 0.01 to 0.05. The standard linear perturbation approach in optical imaging should be augmented to include this nonlinear correction.

This work was supported in part by NASA and the U.S. Army. M. Xu acknowledges support from the U.S. Department of the Army (grant DAMD17-02-1-0516). The authors are indebted to the anonymous referees who helped improve this Letter. M. Xu's e-mail address is minxu@sci.ccnycunyu.edu.

## References

1. A. Yodh and B. Chance, *Phys. Today* **48**(3), 38 (1995).
2. S. R. Arridge, *Inverse Probl.* **15**, R41 (1999).
3. A. H. Gandjbakhche, V. Chernomordik, J. C. Hebden, and R. Nossal, *Appl. Opt.* **37**, 1973 (1998).
4. W. Cai, S. K. Gayen, M. Xu, M. Zavallos, M. Alrubaiee, M. Lax, and R. R. Alfano, *Appl. Opt.* **38**, 4237 (1999).
5. S. Carraresi, T. S. M. Shatir, F. Martelli, and G. Zaccanti, *Appl. Opt.* **40**, 4622 (2001).
6. J. W. Negele and H. Orland, *Quantum Many-Particle Systems* (Westview, Boulder, Colo., 1998).
7. M. Xu, W. Cai, M. Lax, and R. R. Alfano, *Opt. Lett.* **26**, 1066 (2001).
8. W. Cai, M. Lax, and R. R. Alfano, *Phys. Rev. E* **61**, 3871 (2000).
9. A. Guinier, G. Fournet, C. B. Walker, and K. L. Yudowitch, *Small-Angle Scattering of X-Rays* (Wiley, New York, 1955).
10. M. Testorf, U. Osterberg, B. Pogue, and K. Paulsen, *Appl. Opt.* **38**, 236 (1999).
11. M. Xu, W. Cai, M. Lax, and R. R. Alfano, *Phys. Rev. E* **65**, 066609 (2002).
12. H. Rief, *J. Comput. Phys.* **111**, 33 (1994).
13. V. G. Peters, D. R. Wyman, M. S. Patterson, and G. L. Frank, *Phys. Med. Biol.* **35**, 1317 (1990).
14. W. F. Cheong, S. Prahl, and A. J. Welch, *IEEE J. Quantum Electron.* **26**, 2166 (1990).